# 13 C NMR Determination of the Composition of Linear Low-Density Polyethylene Obtained with [η 3 -Methallyl-nickel-diimine]PF 6 Complex

**4 AUTHORS**, INCLUDING:

Griselda Barrera Galland
Universidade Federal do Rio Grande do Sul
**97** PUBLICATIONS **1,658** CITATIONS

SEE PROFILE

Raquel Santos Mauler
Universidade Federal do Rio Grande do Sul
**152** PUBLICATIONS **2,035** CITATIONS

SEE PROFILE

# $^{13}$C NMR Determination of the Composition of Linear Low-Density Polyethylene Obtained with [$\eta^3$-Methallyl-nickel-diimine]PF$_6$ Complex

## Griselda Barrera Galland,* Roberto F. de Souza, Raquel Santos Mauler, and Fernanda F. Nunes

*Instituto de Química, Universidade Federal do Rio Grande do Sul, Av., Bento Gonçalves, 9500, CEP 91501−970, Porto Alegre, Brazil*

*Received October 26, 1998; Revised Manuscript Received December 24, 1998*

ABSTRACT: A complete $^{13}$C NMR characterization of two linear low-density polyethylenes (LLDPE), one highly branched and the other lowly branched, is presented. These LLDPE were synthesized with a new catalyst: the [$\eta^3$-methallyl-nickel-dad]PF$_6$ complex by homopolymerization of ethylene, using different experimental conditions. Methyl, ethyl, propyl, butyl, amyl, and long branches were assigned and quantified.

## Introduction

High-density polyethylene (HDPE), linear low-density polyethylene (LLDPE) obtained from the copolymerization of ethylene with α-olefins, and low-density polyethylene (LDPE) account for 33% of the global thermoplastics industry.[1] Ziegler−Natta catalysts were responsible for the great development of polyolefin industry during the past 40 years. The 1980s witnessed the extraordinary development of the homogeneous catalysts based on group IV metallocenes with methylaluminoxane (MAO) as the cocatalyst.[2] These new catalysts led to polymers with controlled molecular structure, such as narrow distributions of molecular weights and of comonomer composition.[3−6]

Cationic nickel and palladium diimine complexes have been used by Brookhart and co-workers[7,8] in the polymerization of ethylene. These polyethylenes are produced by Du Pont in the Versipol process and have proved to be new highly versatile materials. An advantageous alternative for this catalyst is the $\eta^3$-methallyl-nickel-diimine complexes which have been recently shown as being active with AlEtCl$_2$ replacing MAO as process cocatalysts.[9]

The polyolefinic materials obtained by Brookhart and by us have extensive branching with a consequence of very low density. Polyethylene with densities of 0.85 g cm$^{-3}$ are currently obtained, and a complete characterization of such materials is of enormous scientific and technological importance.

The aim of this work is to determine the microstructure (type and amount of branching) of the VLDPE (very low-density polyethylenes) obtained using the [$\eta^3$-methallyl-nickel-diimine]PF$_6$ (**1**) complex combined with AlEtCl$_2$.

## Experimental Section

The synthesis of the catalyst complex and polymerization reactions were described in a former paper.[9]

The $^{13}$C NMR spectra were obtained at 90 °C for the most branched polymers and at 120 °C for the most linear polymers. The equipment used was a Varian Inova 300 operating at 75 MHz. Sample solutions of the polymer were prepared in *o*-dichlorobenzene and benzene-$d_6$ (20% v/v) in a 5 mm sample tube. The deuterated solvent was used to provide the internal lock signal. The chemical shifts were referenced internally to the major backbone methylene carbon resonance, which was taken as 30.00 ppm from Me$_4$Si. Spectra were taken with a 70° flip angle, an acquisition time of 1.5 s, and a delay of 4.0 s.

**Table 1. Carbon-13 Chemical Shift Calculated, Previous Works, and Observed and Assignments**

| peak no. | calcd | prev works | exptl | assignments |
|---|---|---|---|---|
| 1 | 11.36 | 11.01,[10] 11.209[11] | 11.10 | 1B$_2$ |
| 2 | 13.86 | 14.08,[10] 14.114[11] 14.02,[10] 14.07[11] | 14.12 | 1B$_4$, 1B$_5$, 1B$_n$, 1,4−1B$_n$ |
| 3 | 14.35 | 14.59,[10] 14.0[12] | 14.65 | 1B$_3$ |
| 4 | 19.63 | 20.04,[10] 20.01[11] | 19.90 | 1B$_1$, 1,5-B$_1$, 1,6-B$_1$ |
| 5 | 19,63 | | 19.99 | 1,4-1B$_1$ |
| 6 | 20.21 | 20.15[10] | 20.30 | 2B$_3$ |
| 7 | 22.65 | 22.88,[10] 22.8[12] 22.84,[10] 22.88[11] | 22.88 | 2B$_5$ 2B$_n$ 1,4-2B$_n$ |
| 8 | 22.90 | 23.36,[10] 23.38[11] | 23.37 | 2B$_4$ |
| 9 | 24.58 | 24.65,[13] 24.85[10] | 24.61 | 1,5-$\beta'$B$_1$ |
| 10 | 27.16 | 26.789[11] | 26.51 | 2B$_2$ |
| 11 | 27.52 | 27.35,[11] 27.3[12] 27.33[10,11] | 27.20 | $\beta$B$_2$ $\beta$B$_3$, $\beta$B$_4$, $\beta$B$_5$, $\beta$B$_n$, $(n$−1$)$B$_n$, 1,4-$\beta$B$_n$, 1,4-$(n$−1$)$B$_n$ |
| 12 | 27.27 | 27.45[11] 27.3[12] | 27.42 | $\beta$B$_1$ 1,4-$\beta$B$_1$, 1,5-$\beta$B$_1$, 1,6-$\beta$B$_1$ 4B$_5$ |
| 13 | 27.52 | 27.85[12] | 27.79 | 1,6-$\beta'$B$_1$ |
| 14 | 29.96 | 29.55[13] | 29.38 | 3B$_4$ |
| 15 | 29.71 | 29.536[13] | 29.59 | 4B$_n$ 1,4-4B$_n$ |
| 16 | 29.96 | 30.00[10,11] | 30.00 | $\delta$B$_{1-n}$ |
| 17 | 30.21 | 30.38[11] | 30.36 | $\gamma$B$_1$ 1,4-$\gamma$B$_1$, 1,5-$\gamma$B$_1$, 1,6-$\gamma$B$_1$ |
| 18 | 30.21 | 30.50[11] 30.476[13] | 30.48 | $\gamma$B$_2$, $\gamma$B$_4$ $\gamma$B$_3$, $\gamma$B$_5$, 1,4-$\gamma$B$_n$, 1,4-$(n$−2$)$B$_n$ $\gamma$B$_n$ |
| 19 | 32.03 | | 31.50 | 1,4-$\alpha'$B$_n$ |
| 20 | 32.40 | 32.18,[10] 32.21[11] | 32.16 | 3B$_n$ 1,4-3B$_n$ |
| 21 | 32.65 | 32.70,[10] 32.8[12] | 32.65 | 3B$_5$ |
| 22 | 32.52 | 33.26,[11] 33.1[12] | 33.14 | brB$_1$ 1,5-brB$_1$, 1,6-brB$_1$ |
| 23 | 32.52 | | 33.409, 33.476, 33.543 | 1,4-brB$_1$ |
| 24 | 34.22 | 34.13,[11] 34.118[13] | 33.83 | $\alpha$B$_2$ |
| 25 | 34.22 | 34.22,[10] 34.20[11] | 33.94 | 4B$_4$ |
| 26 | 34.47 | 34.60[11] 34.7[12] 34.61,[10] 34.7[12] | 34.39 | $\alpha$B$_3$ $\alpha$B$_4$ 5B$_5$ $\alpha$B$_5$, $\alpha$B$_n$, $n$B$_n$ 1,4-$\alpha$B$_n$, 1,4-$n$B$_n$ |
| 27 | 34.22 | r-35.7/m-34.9[12] | 34.731, 34.785 | 1,4-$\alpha'$B$_1$ |
| 28 | 36.91 | | 36.72 | 3B$_3$ |
| 29 | 36.91 | 37.56[11] | 37.47 | $\alpha$B$_1$ 1,4-$\alpha$B$_1$, 1,5-$\alpha$B$_1$, 1,6-$\alpha$B$_1$, 1,6-$\alpha'$B$_1$ |
| 30 | 37.05 | r-38.8/m-37.96[12] | 37.8 | brB$_3$ |
| | 37.16 | | | 1,5-$\alpha'$B$_1$ |
| 31 | 37.05 | 38.23,[10] 38.19[11] 38.23[10] 38.23,[10] 38.24[11] | 37.99 | brB$_4$ brB$_5$ brB$_n$ |
| 32 | 37.05 | | 38.24 | 1,4-brB$_n$ |
| 33 | 39.12 | 39.75[10,11] | 39.44 | brB$_2$ |

Polyethylenes used in this work have the following properties: Polyethylene of Figure 1a: mp = 133 °C, $M_w$ = 20.0 × 10$^4$ g/mol, $M_n$ = 7.9 × 10$^4$ g/mol, $X_c$ = 54%. Polyethylene of Figure 1b: mp = 113 °C, $M_w$ = 40.0 × 10$^4$ g/mol, $M_n$ = 16.0 ×
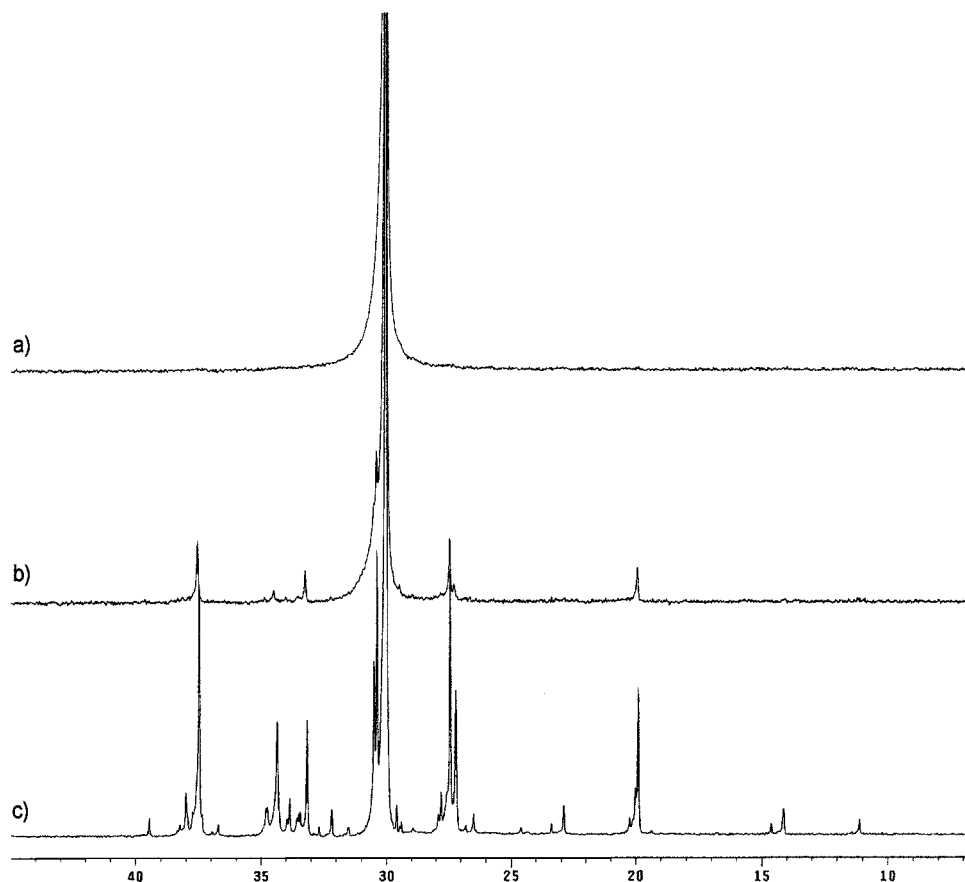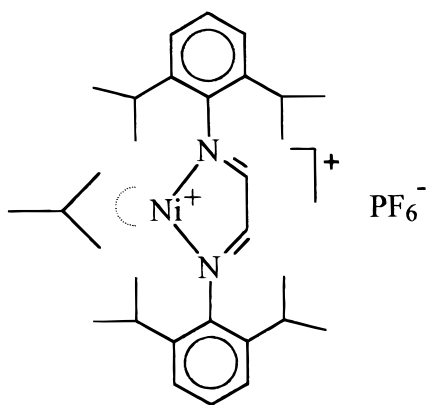
**Figure 1.** (a) $^{13}$C NMR spectrum of polyethylene synthesized at the following polymerization conditions: 0 °C, $P_E$ = 15 atm, Al/Ni = 10, solvent = PhCl. (b) $^{13}$C NMR spectrum of polyethylene synthesized at the following polymerization conditions: 0 °C, $P_E$ = 1 atm, Al/Ni = 10, solvent = PhCl. (c) $^{13}$C NMR spectrum of polyethylene synthesized at the following polymerization conditions: 20 °C, $P_E$ = 1 atm, Al/Ni = 100, solvent = PhCl.



$10^4$ g/mol, $X_c$ = 31%. Polyethylene of Figure 1c: mp = 93 °C, $M_w$ = 11.2 × $10^4$ g/mol, $M_n$ = 5.3 × $10^4$ g/mol, $X_c$ = 11%.

## Results and Discussion

$^{13}$C NMR spectra of polyethylenes obtained by homopolymerization of ethylene with [$\eta^3$-methallyl-nickel-dad]PF$_6$ with different branching can be seen in Figure 1. Depending on experimental conditions, it is possible to obtain from a high linear homopolymer (Figure 1a) to a high branched linear low-density polyethylene (Figure 1c). The microstructure determination of a highly branched polyethylene (Figure 2) is shown in Table 1. The assignments were based on APT-$^{13}$C spectra (Figure 3), theoretical chemical shifts calculated by Linderman and Adams,[10] and previous assignments.[11−15]

Nomenclature used in this work is that of Usami and Takayama[11] for isolated branches. Branches are named by $xB_n$, where $n$ is the length of the branch and $x$ is the carbon number starting with the methyl group as "1". For the backbone carbons, Greek letters and "br" are used instead of $x$ for the methylenes and a branch point, respectively. For example, 1B$_1$ designates the methyl in a methyl branch, 2B$_2$ the methylene carbon in an ethyl branch, and $\gamma$B$_2$ the backbone carbon in the $\gamma$-position from an ethyl branch.
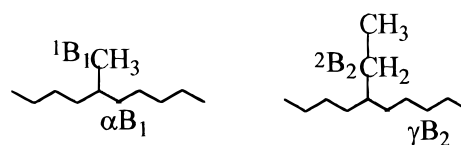


For paired branches prefixes 1,$m$ is used, where $m$ is the number of carbons between two tertiary carbons, 1 being the first tertiary carbon and $m$ the next. The backbone carbons between branches are designated by Greek letters with primes.
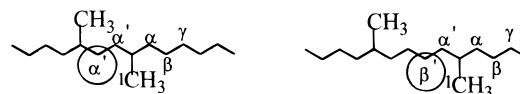


Circled carbon is 1,4-$\alpha$'B$_1$          Circled carbon is 1,6-$\beta$'B$_1$

Methyl carbon is 1,4-1B$_1$          Methyl carbon is 1,6-1B$_1$

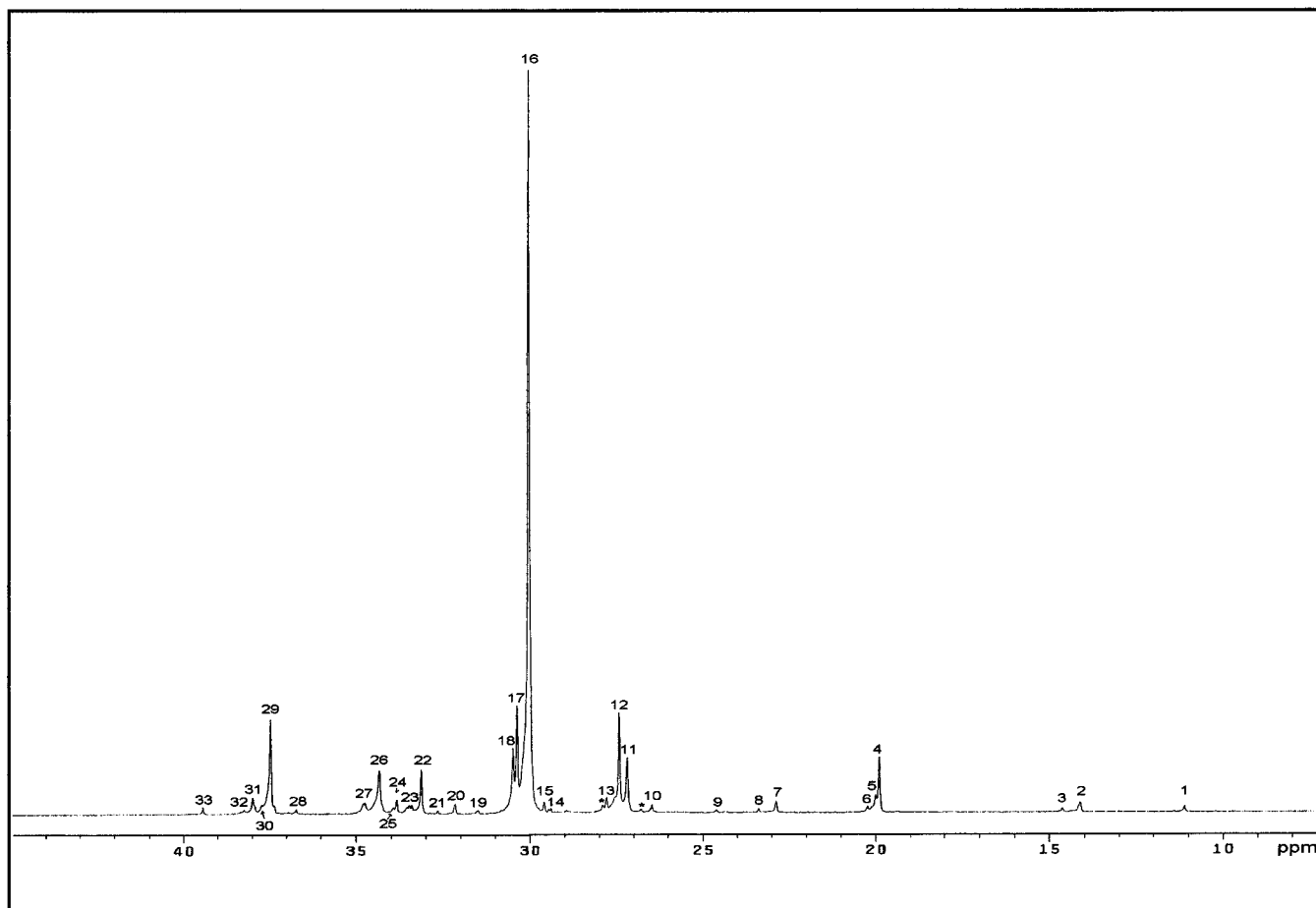Paired branches were found only for branches of the same size.

**Figure 2.** ^{13}C NMR spectrum of polyethylene synthesized at the following polymerization conditions: 20 °C, $P_E = 1$ atm, Al/Ni = 100, solvent = PhCl. Peaks marked with an asterisk were not assigned.

**Methyl Branches.** The assignments for methyl isolated branches do not differ significantly from other studies.[11-15] Paired 1,2 and 1,3 methyl branches were not found since resonances close to 16.64 and 40 ppm, from 1,2-1B$_1$ and 1,3-$\alpha'$B$_1$ carbons, respectively, were not present. Paired 1,4 methyl branches were identified by the presence of the resonances at 19.99 ppm of 1,4-1B$_1$ carbon, the resonances at 33.543, 33.476, and 33.409 ppm corresponding to the 1,4-brB$_1$ carbon, and the resonances at 34.785 and 34.731 ppm corresponding to the 1,4-$\alpha'$B$_1$ carbon. The resonances of 1,4-brB$_1$ and 1,4-$\alpha'$B$_1$ are split due to the presence of meso and racemic structures. These splittings were not reported in previous works. Paired 1,5 methyl branches were identified by the resonance of the 1,5-$\beta'$B$_1$ carbon at 24.61 ppm.

The presence of 1,6 paired methyl branches was confirmed by the resonance of the 1,6-$\beta'$B$_1$ carbon at 27.79 ppm, and the other resonances are superimposed.

The absence of 1,7 paired methyl branches is suggested by the absence of the 1,7-$\gamma'$B$_1$ resonance assigned by Cheng[13] at 30.8 ppm.

Methyl branches with spacings longer than seven carbons appear as isolated branches.

**Short Branches.** The presence of short branches as ethyl, butyl, and amyl was identified by the resonances of specific carbons (Figure 2 and Table 1). Due to the low content of these branches (see intensities), the existence of short paired branches seems improbable, and in fact, these branches were not found. We had some difficulty assigning resonances at 27.20 and 27.42 ppm since calculated chemical shift for $\beta$B$_1$ resonances

(isolated and paired) is 27.27 ppm and for $\beta$B$_{2+}$ is 27.52 ppm, but integrals do not agree with this assignment as we had more methyl branches than the others. On the basis of De Pooter's work[12] and our copolymer spectra, the lower field peak was assigned to $\beta$B$_1$ (isolated and paired) carbons and the higher field to $\beta$B$_{2+}$ carbons.

In previous works[13-15] no differences between 4B$_5$ and $\beta$B$_5$ were observed, and it is claimed that their resonance is at 27.3 ppm. Cavagna[16] showed that it is possible to distinguish between 5B$_6$ and $\beta$B$_6$ resonances in ethylene-1-octene copolymers at 67.9 MHz, their separation amounting to 0.027 ppm. On the basis of that, the difference between $\beta$B$_5$ and 4B$_5$ should be even higher since branches are more influenced by the branch chain end, as they are shorter than hexyl branches. This reasoning led us to assign resonances at 27.42 ppm to 4B$_5$ and at 27.20 ppm to $\beta$B$_5$ where they are superimposed to others.

**Long Branches.** The most surprising feature in this work was the presence of a good number of long branches ($n \geq 6$). These branches are confirmed by the presence of 3B$_n$ and 4B$_n$ at 32.16 and 29.59 ppm, respectively. Due to the high content of these branches, it seems reasonable to identify the 1,4 paired branches by the resonances at 31.50 and 38.24 ppm assigned to the carbons 1,4-$\alpha'$B$_n$ and 1,4-brB$_n$.

Other authors[11,14,17] reported that it is possible to distinguish between 3B$_6$ and 3B$_{n>6}$ and between 1B$_6$ and 1B$_{n>6}$. The resonance peak at 32.17 ppm would show a splitting corresponding to the resonance at
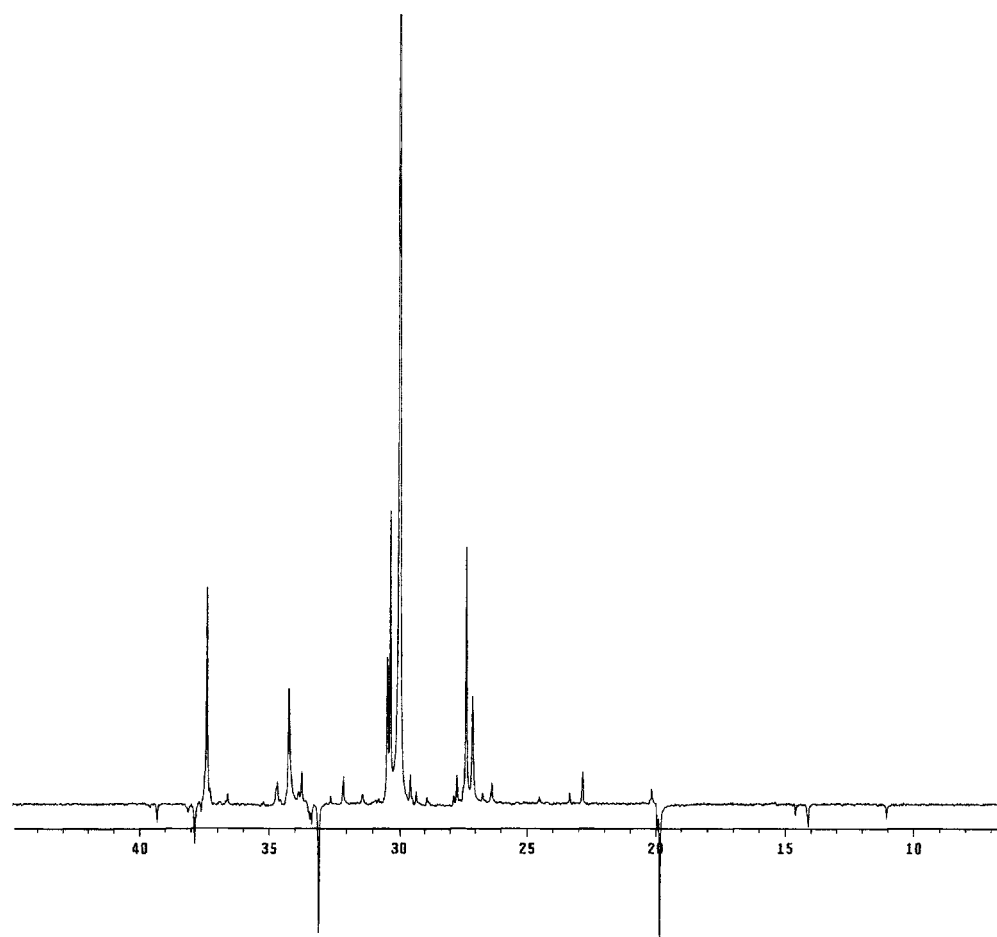
**Figure 3.** APT-$^{13}$C spectrum of polyethylene synthesized at the following polymerization conditions: 20 °C, $P_E = 1$ atm, Al/Ni = 100, solvent = PhCl.

**Table 2. Calculated and Experimental Integrals, Percentage of Branching over Total Branching and over Total Polymer of Figure 1a**

| 13C-NMR QUANTITATIVE DETERMINATION | | | | NAME: ROB49 | | Percentage over total branching | Percentage of branching |
|---|---|---|---|---|---|---|---|
| Peak No. | Chem Shift (ppm) | Integral calc. | Integral exp. | Branch content | | | |
| 1 | 11.10 | 0.10 | 0.07 | $N_M$ | 0.323 | 34.10% | 5.14% |
| 2 | 14.12 | 0.22 | 0.18 | $N_{M\,(1.4)}$ | 0.158 | 16.65% | 2.51% |
| 3 | 14.65 | 0.05 | 0.05 | $N_{M\,(1.5)}$ | 0.040 | 4.23% | 0.64% |
| 4 | 19.90 | 0.59 | 0.59 | $N_{M\,(1.6)}$ | 0.095 | 10.04% | 1.51% |
| 5 | 19.99 | 0.32 | 0.22 | $N_E$ | 0.098 | 10.40% | 1.57% |
| 6 | 20.30 | 0.05 | 0.06 | $N_P$ | 0.050 | 5.29% | 0.80% |
| 7 | 22.88 | 0.15 | 0.15 | $N_B$ | 0.065 | 6.87% | 1.04% |
| 8 | 23.37 | 0.07 | 0.04 | $N_A$ | 0.030 | 3.17% | 0.48% |
| 9 | 24.61 | 0.04 | 0.04 | $N_L$ | 0.055 | 5.81% | 0.88% |
| 10 | 26.51 | 0.10 | 0.13 | $N_{L\,(1.4)}$ | 0.033 | 3.44% | 0.52% |
| 11 | 27.20 | 0.78 | 0.83 | $\delta\delta CH_2$ | 10.65 | 100% | 15.08% |
| 12 | 27.42 | 1.26 | 1.57 | [E] | 5.33 | | |
| 13 | 27.79 | 0.19 | 0.19 | [R] | 0.95 | | |
| 14 | 29.38 | 0.07 | | Total branching | **15.08%** | Polymer branching | |
| 15 | 29.59 | 0.12 | 0.12 | | | | |
| 16 | 30.00 | 10.77 | 10.77 | Methyl branches | | 9.81% | |
| 17 | 30.36 | 1.23 | 1.57 | Ethyl branches | | 1.57% | |
| 18 | 30.48 | 0.78 | 0.9 | Propyl branches | | 0.80% | |
| 19 | 31.50 | 0.07 | 0.06 | Butyl branches | | 1.04% | |
| 20 | 32.16 | 0.12 | 0.12 | Amyl branches | | 0.48% | |
| 21 | 32.65 | 0.03 | 0.03 | Long branches | | 1.40% | |
| 22 | 33.14 | 0.59 | 0.55 | | Total= | 15.08% | |
| 23 | 33.48 | 0.32 | 0.28 | | | | |
| 24 | 33.83 | 0.20 | 0.17 | | | | |
| 25 | 33.94 | 0.07 | 0.09 | | | | |
| 26 | 34.39 | 0.62 | 1.06 | | | | |
| 27 | 34.75 | 0.32 | 0.35 | | | | |
| 28 | 36.72 | 0.05 | 0.05 | | | | |
| 29 | 37.47 | 1.42 | 1.42 | | | | |
| 30 | 37.80 | 0.13 | | | | | |
| 31 | 37.99 | 0.15 | 0.27 | | | | |
| 32 | 38.24 | 0.07 | 0.07 | | | | |
| 33 | 39.44 | 0.10 | 0.08 | | | | |

**Table 3. Calculated and Experimental Integrals, Percentage of Branching over Total Branching and over Total Polymer of Figure 1b**

| 13C-NMR QUANTITATIVE DETERMINATION | | | | NAME: ROB27 | | Percentage over total branching | Percentage of branching |
|---|---|---|---|---|---|---|---|
| Peak No. | Chem Shift (ppm) | Integral calc. | Integral exp. | Branch content | | | |
| 1 | 11.10 | 0.73 | 1 | $N_M$ | 4.910 | 47.26% | 1.35% |
| 2 | 14.12 | 1.97 | 0.61 | $N_{M\,(1.4)}$ | 1.110 | 10.69% | 0.30% |
| 3 | 14.65 | 0 | 0 | $N_{M\,(1.5)}$ | 0.000 | 0.00% | 0.00% |
| 4 | 19.90 | 8.25 | 9.48 | $N_{M\,(1.6)}$ | 1.670 | 16.08% | 0.46% |
| 5 | 19.99 | 2.22 | 1.79 | $N_E$ | 0.728 | 7.01% | 0.20% |
| 6 | 20.30 | 0.00 | 0 | $N_P$ | 0.000 | 0.00% | 0.00% |
| 7 | 22.88 | 1.97 | 0.77 | $N_B$ | 0.000 | 0.00% | 0.00% |
| 8 | 23.37 | 0.00 | 0 | $N_A$ | 0.000 | 0.00% | 0.00% |
| 9 | 24.61 | 0.00 | 0 | $N_L$ | 1.97 | 18.96% | 0.54% |
| 10 | 26.51 | 0.73 | 0.72 | $N_{L\,(1.4)}$ | 0.000 | 0.00% | 0.00% |
| 11 | 27.20 | 7.37 | 5.23 | $\delta\delta CH_2$ | 708.200 | 100% | 2.85% |
| 12 | 27.42 | 15.38 | 17.55 | [E] | 354.10 | | |
| 13 | 27.79 | 3.34 | 3.34 | [R] | 10.39 | | |
| 14 | 29.38 | 0.00 | 0 | Total branching | **2.85%** | | |
| 15 | 29.59 | 1.97 | 4.34 | | | | |
| 16 | 30.00 | 710.17 | 710.17 | Methyl branches | | 2.11% | |
| 17 | 30.36 | 15.38 | 17.55 | Ethyl branches | | 0.20% | |
| 18 | 30.48 | 7.37 | 7.4 | Propyl branches | | 0.00% | |
| 19 | 31.50 | 0.00 | 0 | Butyl branches | | 0.00% | |
| 20 | 32.16 | 1.97 | 1.97 | Amyl branches | | 0.00% | |
| 21 | 32.65 | 0.00 | 0 | Long branches | | 0.54% | |
| 22 | 33.14 | 8.25 | 7.23 | | | 2.85% | |
| 23 | 33.48 | 2.22 | 3.12 | | | | |
| 24 | 33.83 | 1.46 | 1.47 | | | | |
| 25 | 33.94 | 0.00 | 0 | | | | |
| 26 | 34.39 | 5.91 | 4.11 | | | | |
| 27 | 34.75 | 2.22 | 1.32 | | | | |
| 28 | 36.72 | 0.00 | 0 | | | | |
| 29 | 37.47 | 18.72 | 18.72 | | | | |
| 30 | 37.80 | 0.00 | 0 | | | | |
| 31 | 37.99 | 1.97 | 1.9 | | | | |
| 32 | 38.24 | 0.00 | 0 | | | | |
| 33 | 39.44 | 0.73 | 0.73 | | | | |

32.191 ppm to $3B_6$ and at 32.156 ppm to $3B_{n>6}$, and the resonance peak at 14.0 ppm would show also a splitting corresponding to the resonance at 14.024 ppm to $1B_6$ and at 14.003 ppm to $1B_{n>6}$. We noticed no splitting of these peaks in our spectra, so we conclude that $B_n$ branches in this sample correspond mainly to branches with $n > 6$.

**Quantitative Analysis.** The main problems of quantitative analysis are different spin–lattice relaxation times and NOE of nonequivalent carbons. These problems can be avoided by the use of long delay times or gated decoupling or by the addition of paramagnetic reagents.[3,4,12,18–20] However, these techniques lower experimental efficiency in terms of the time required to obtain a spectrum. It was also shown[21] that signal/noise decreases with increasing integral accuracy. Thus, a good spectral resolution does not go in the same direction as integral accuracy. It is necessary to make a compromise between these two factors.

Traficante[21] described a procedure that allows a determination of the S/N for various integral accuracies. The use of an integral accuracy of 90% instead of 100% increases S/N by 31%. The use of a pulse angle of 70° instead of 90° permits the pulse delay to be reduced from $5T_1$ to $1.6T_1$ with an integral accuracy of 85%. The $T_1$ values for most of the carbons in these samples are less than 2.0 s, and therefore, a delay time of only 4 s would be sufficient. Methyl and some branch carbons that have longer $T_1$ values should be neglected. The NOE is generally assumed complete and identical for all carbons in PE.[19] Hansen[14] measured NOE for each carbon atom in LDPE and found that approximately half of the resonance lines reveal a theoretical maximum NOE factor of 2.98, while more than 25% of the peaks exhibit a NOE factor of less than 2.75 s. However, when he determined different branch average numbers and distribution, the branch numbers derived from NOE experiments were in surprisingly good agreement with corresponding branch numbers derived from "no NOE" experiments. On the basis of this previous work, we decided to invest in a good resolution spectrum made in the minimum possible time. We used conditions of full NOE, Pw = 70, AT = 1.5, and pulse delay of 4 s. In all cases, when it was possible, we neglected the resonances of carbons with $T_1$ longer than 2 s. In some cases it was necessary to use these peaks for an estimate branch content because there were no other possibilities. A list of the number of branches corresponding to each peak is summarized below, $k$ being the normalization constant. The symbols $N_M$, $N_E$, $N_P$, $N_B$, $N_A$, and $N_L$ represent the branch content of methyl, ethyl, propyl, butyl, amyl, and longer ($n \geq 6$) branches, respectively. The paired branches are indicated by a suffix placed by the branch type. For example, $N_{M(1,5)}$ means the branch content of paired 1,5 methyl–methyl branches.

$$I_1 = kN_E$$

$$I_2 = k(N_B + N_A + N_L + 2N_{L(1,4)})$$

$$I_3 = kN_P$$

$$I_4 = k(N_M + 2N_{M(1,5)} + 2N_{M(1,6)})$$

$$I_5 = k(2N_{M(1,4)})$$

$$I_6 = kN_P$$

$$I_7 = k(N_A + N_L + 2N_{L(1,4)})$$

$$I_8 = kN_B$$

$$I_9 = kN_{M(1,5)}$$

$$I_{10} = kN_E$$

$$I_{11} = k(2N_E + 2N_P + 2N_B + 2N_A + 3N_L + 4N_{L(1,4)})$$

$$I_{12} = k(2N_M + 2N_{M(1,4)} + 2N_{M(1,5)} + 2N_{M(1,6)} + N_A)$$

$$I_{13} = k2N_{M(1,6)}$$

$$I_{14} = k(N_B)$$

$$I_{15} = k(N_L + 2N_{L(1,4)})$$

$$I_{16} = \text{main chain}$$

$$I_{17} = k(2N_M + 2N_{M(1,4)} + 2N_{M(1,5)} + 2N_{M(1,6)})$$

$$I_{18} = k(2N_E + 2N_P + 2N_B + 2N_A + 3N_L + 4N_{L(1,4)})$$

$$I_{19} = k2N_{L(1,4)}$$

$$I_{20} = k(N_L + 2N_{L(1,4)})$$

$$I_{21} = kN_A$$

$$I_{22} = k(N_M + 2N_{M(1,5)} + 2N_{M(1,6)})$$

$$I_{23} = k2N_{M(1,4)}$$

$$I_{24} = k2N_E$$

$$I_{25} = kN_B$$

$$I_{26} = k(2N_P + 2N_B + 3N_A + 3N_L + 4N_{L(1,4)})$$

$$I_{27} = k2N_{M(1,4)}$$

$$I_{28} = kN_P$$

$$I_{29} = k(2N_M + 2N_{M(1,4)} + 2N_{M(1,5)} + 4N_{M(1,6)})$$

$$I_{30} = k(N_P + 2N_{M(1,5)})$$

$$I_{31} = k(N_B + N_A + N_L)$$

$$I_{32} = k2N_{L(1,4)}$$

$$I_{33} = kN_E$$

From these equations it is possible to obtain the following relations directly (being $k = 1$):

$$N_E = (I_{10} + I_{24}/2 + I_{33})/3$$

$$N_P = I_{28}$$

$$N_B = (I_8 + I_{25})/2$$

($I_8$ $T_1$ long, $I_{25}$ superimposed, estimated)

$$N_A = I_{21}$$

$$N_{M(1,5)} = I_9$$

$$N_{M(1,4)} = (I_{23}/2 + I_{27}/2)/2$$

$$N_{M(1,6)} = I_{13}/2$$

$$N_{L(1,4)} = (I_{19}/2 + I_{32}/2)/2$$

The branch content above can be obtained directly from the $^{13}$C NMR resonances. The following branches content can be obtained from the equations above:

$$N_L = (I_{15} - 2N_{L(1,4)}) = (I_{20} - 2N_{L(1,4)})$$

$$= I_{15} - (I_{19}/2 + I_{32}/2) = I_{20} - (I_{19}/2 + I_{32}/2)$$

($I_{15}$ and $I_{20}$ have a long $T_1$, estimated)

$$N_M = (I_{22} - (2N_{M(1,6)} + 2N_{M(1,5)}) = (I_{29} - (2N_{M(1,4)} + 4N_{M(1,6)} + 2N_{M(1,5)}))/2$$

$$= (I_{12} - (2N_{M(1,4)} + 2N_{M(1,6)} + N_A + 2N_{M(1,5)}))/2$$

$$= I_{22} - (I_{13} + 2I_9) = (I_{29} - (I_{23}/2 + I_{27}/2 + 2I_{13} + 2I_9)/2$$

$$= (I_{12} - (I_{23}/2 + I_{27}/2 + I_{13} + I_{21} + 2I_9)/2$$

Tables 2 and 3 show the experimental integrals of the

$$\text{total methyl branches} = N_M + N_{M(1,4)} + N_{M(1,5)} + N_{M(1,6)}$$

$$\text{total long branches} = N_L + N_{L(1,4)}$$

spectra of Figure 1, c and b, respectively: the calculated integrals obtained from equations above and the percentages of each type of branch. From these results, the polyethylene in Figure 1c consists of 9.8% methyl branches, 1.6% ethyl branches, 0.8% propyl branches, 1.0% butyl branches, 0.5% amyl branches, and 1.4% long branches ($n \geq 6$). The total amount of branching is 15.1%. The LLDPE in Figure 1b consists of 2.1% methyl branches, 0.2% ethyl branches, and 0.5% long branches. The total amount of branching is 2.8%.

These are estimated results because the spectra were not taken in perfect quantitative conditions (100%) of integral accuracy. Despite that, the experimental and calculated integral peaks do not differ appreciably (Tables 2 and 3). The major differences between experimental and calculated integrals are mainly due to those resonances where $T_1$ is longer than 2 s.

The amount of branching type follows in both cases the following order:

$$\text{methyl} \gg \text{ethyl} \cong \text{long} > \text{butyl} \cong \text{propyl} > \text{amyl}$$

In the polymer with 2.85% branching butyl, propyl, and amyl branches are not presented.

## Conclusion

The homopolymerization of ethylene with [$\eta^3$-methallyl-nickel-dad]PF$_6$ complex leads to polyethylene, from highly linear to highly branched, depending on experimental conditions. The branches are formed mainly by isolated methyl groups. When concentration of branches is high, some paired methyl–methyl branches are found, especially 1,4- and 1,6-B$_1$. There are only small amounts of other branches which are mainly ethyl and long branches. The presence of long branches makes this synthesis very interesting as it is known that these branches improve rheological properties, which facilitates the processing of these polymers. The implication of the branch distribution on the polymerization mechanism is discussed in a another paper.[22]

## References and Notes

(1) Olabisi, O.; Atiqullah, M.; Kaminsky, W. *J. Macromol. Sci., Rev. Macromol. Chem. Phys.* **1997**, *C37* (3), 519–554.
(2) Montagna, A. A.; Dekmezian, A. H.; Burkhart, R. M. *Chemtech* **1997**, 26–31.
(3) Galland, G. B.; Quijada, R.; Mauler, R. S.; Menezes, S. C. de. *Macromol. Rapid Commun.* **1996**, *17*, 607–613.
(4) Galland, G. B.; Mauler, R. S.; Menezes, S. C. de; Quijada, R. *Polym. Bull.* **1995**, *34*, 599–604.
(5) Quijada, R.; Rojas, R.; Mauler, R. S.; Galland, G. B.; Scipioni, R. J. *Appl. Polym. Sci.* **1997**, *64*, 2567–2574.
(6) Quijada, R.; Galland, G. B.; Mauler, R. S. *Macromol. Chem. Phys.* **1996**, *197*, 3091–3098.
(7) Johnson, L. K.; Killian, C. M.; Brookhart, M. *J. Am. Chem. Soc.* **1995**, *117*, 6414–6415.
(8) McLain, S. J.; McCord, E. F.; Johnson, L. K.; Ittel, S. D.; Nelson, L. T. J.; Arthur, S. D.; Halfhill, M. J.; Teasley, M. F.; Tempel, D. J.; Killian, C.; Brookhart, M. S. *ACS Polym. Prepr.* **1997**, *38* (1), 772–773.
(9) Souza, R. F. de; Mauler, R. S.; Simon, L. C.; Nunes, F. F.; Vescia, D. V.; Cavagnolli, A. *Macromol. Rapid Commun.* **1997**, *18*, 795–800.
(10) Linderman, L. P.; Adams, N. O. *Anal. Chem.* **1971**, *43* (10), 1245–1252.
(11) Usami, T.; Takayama, S. *Macromolecules* **1984**, *17*, 1756–1761.
(12) De Pooter, M.; Smith, P. B.; Dohrer, K. K.; Bennett, K. F.; Meadows, M. D.; Smith, C. G.; Schouwenaars, H. P.; Geerards, R. A. *J. Appl. Polym. Sci.* **1991**, *42*, 399–408.
(13) Cheng, H. N. *Polym. Bull.* **1986**, *16*, 445–452.
(14) Hansen, E. W.; Blom, R.; Bade, O. M. *Polymer* **1997**, *38* (17), 4295–4304. (b) Hansen, E. W.; Redford, K.; Oysaed, H. *Polymer* **1996**, *37* (1), 19–24.
(15) Randall, J. C. *Rev. Macromol. Chem. Phys.* **1989**, *C29* (2&3), 201–317.
(16) Cavagna, F. *Macromolecules* **1981**, *14*, 215–216.
(17) Bugada, D. C.; Rudin, A. *Eur. Polym. J.* **1987**, *23*, 809–818.
(18) Axelson, D. E.; Levy, G. C.; Mandelkern, L. *Macromolecules* **1979**, *12* (1), 41–52.
(19) Bovey, F. A. In *Nuclear Magnetic Resonance Spectroscopy*, 2nd ed.; Academic Press: London, 1988.
(20) Abraham, R. J.; Loftus, P. In *Proton and Carbon-13 NMR Spectroscopy*; Heiden: London, 1979.
(21) Traficante, D. D.; Steward, L. R. *Concepts Magn. Reson.* **1994**, *6*, 131–135.
(22) Souza, R. F. de; Mauler, R. S.; Nunes, F. F. *Macromol. Chem. Phys.*, submitted for publication.

MA981669H